J. Applied Membrane Science & Technology, Vol. 30, August 2026, 96-111
©Universiti Teknologi Malaysia

Development of Zeolitic Imidazolate Framework-8/Polydimethylsiloxane Membrane with Primitive Structure for Carbon Dioxide Permeation Study

Jin Xuan Lee[1], Linggao Shi[1,2], Kok Bin Low[1], Wee Horng Tay[3], Jing Yao Sum[1], Li Sze Lai[1,4*]

[1]Department of Chemical & Petroleum Engineering, Faculty of Engineering, Technology and Built Environment, UCSI University, Kuala Lumpur, Malaysia
[2]School of Medical Science, Guangxi University of Science and Technology, 545006 Guangxi, China
[3]Gensonic Technology, Persiaran SIBC 12, Seri Iskandar Business Centre, 32610 Seri Iskandar, Malaysia
[4]UCSI-Cheras Low Carbon Innovation Hub Research Consortium, Kuala Lumpur, Malaysia

Submitted: 18/05/2026. Revised edition: 03/07/2026. Accepted: 06/07/2026. Available online: 21/08/2026

ABSTRACT
Membrane technology plays a vital role in carbon dioxide (CO_2) removal as one of the key actions to mitigate climate change. Additive manufacturing has emerged as an alternative method for membrane fabrication due to its high flexibility. Triply periodic minimal surface (TPMS) architectures are widely recognized for their high mechanical robustness and distinctive properties with continuous smooth geometry and zero mean curvature. These features facilitate seamless fluid flow across the structure, and thus, minimizing stagnant regions and reducing the risk of contamination. Among the TPMS structures, the primitive structure is notable for its high compressive strength and mechanical resistance. This study aims to fabricate and evaluate a primitive-structured zeolitic imidazolate framework-8 (ZIF-8)/polydimethylsiloxane (PDMS) mixed-matrix membrane with 2 × 1 × 1 cubic unit cell for carbon dioxide permeation using a sacrificial mold fabrication approach. The membrane was fabricated using a sacrificial mold printed via fused deposition modeling. The ZIF-8 fillers and membranes were characterized using field emission scanning electron microscopy (FESEM) with energy-dispersive X-ray spectroscopy (EDX), Fourier-transform infrared spectroscopy (FTIR), differential scanning calorimetry (DSC), and thermogravimetric analysis (TGA). The primitive-structured ZIF-8/PDMS membrane demonstrated CO_2 permeability and CO_2/N_2 ideal selectivity that are comparable to reported literature values, reaching $13.17 \pm 0.57 \times 10^3$ Barrer and 7.76 ± 0.28, respectively, at 0.025 bar. This suggests that removing the sacrificial mold through dissolution is unlikely to compromise the membrane surface, and therefore, represents a viable approach for the fabrication of membranes with complicated structures.

Keywords: ZIF-8 nanoparticles, ZIF-8/PDMS membrane, TPMS, Primitive structure, CO_2 gas permeation, Additive manufacturing

* Corresponding to: Li Sze Lai (email: LaiLS@ucsiuniversity.edu.my)
DOI: https://doi.org/10.11113/jamst.v30n2.346

1.0 INTRODUCTION

Nowadays, greenhouse gas emissions have increased, resulting in several serious environmental issues due to the greenhouse effect [1, 2]. Carbon dioxide (CO_2) is the primary greenhouse gas responsible for global warming. There are several methods for removing CO_2 from the gas mixture, such as alkanolamine absorption schemes, adsorption, chemisorption, membrane technology, cryogenic processes, and enzymatic processes [3]. Membrane technology has been selected for this study because it offers high selectivity for CO_2 removal [4]. Typically, the types of membranes that can be used for the removal of CO_2 include polymeric, inorganic, and mixed-matrix. The mixed-matrix membrane combines the favorable characteristics of both polymeric and inorganic materials, resulting in the improved selectivity, permeability, stability, and membrane performance beyond what is achievable with either component alone [5]. By adjusting the ratio and types of components, mixed-matrix membranes can be tailored to exhibit specific properties, such as pore size, surface chemistry, and mechanical strength [6].

Zeolitic imidazolate framework-8, also known as ZIF-8, has a high tuneable ability for various industrial processes due to its high thermal and chemical stabilities. It is also highly potential in separating CO_2 from other mixed gas attributed to its small apertures of ~0.34 nm [7]. Polydimethylsiloxane (PDMS) membranes have been studied for their potential to be used in CO_2 separation [8]. It offers a surface with good gas permeability [9], strong thermal stability, low interfacial free energy, chemical inertness, and optical transparency. Taherizadeh *et al.* developed PDMS/SSZ-13 composite membrane for CO_2/CH_4 separation [10]. The membrane showed CO_2 permeance up to 23.8×10^{-7} mol/m^2 s Pa and an ideal CO_2/CH_4 selectivity of 207.75. Wang and co-workers successfully developed PDMS/UiO-66-NH_2 membrane for CO_2/N_2 separation. The membrane was reported to have CO_2 permeability of 2586 barrer and CO_2/N_2 ideal selectivity of 18 [11]. ZIF-8-CNT-PDMS membrane has been developed for CO_2/N_2 separation [8]. The membrane showed exceptionally high CO_2 permeability up to 8705 barrer and CO_2/N_2 selectivity of 45.6. Fu *et al*. have also fabricated a composite membrane with a ZIF-8-doped PDMS active layer on a mullite-based substrate. The membrane showed high CO_2 permeance of 4.58×10^4 barrer and CO_2/N_2 selectivity of 10.7 [12]. For additive manufacturing of membrane, Gutierrez *et al.* fabricated a PDMS-based membranes for CO_2/N_2 separation via direct ink writing [13]. Silica (SiO_2) particles were added to introduce thixotropy and produce a non-flowing PDMS-based ink. The membrane demonstrated high CO_2 permeability of 5202.10 barrer and CO_2/N_2 selectivity of 10.50.

Triply Periodic Minimal Surface (TPMS) is one of the membrane geometries characterized by intricate geometric patterns. Unlike flat sheets or hollow fiber structures, TPMS represent complex three-dimensional structures with interconnected pores arranged in a periodic lattice. This membrane geometry is beneficial in various application due to its mass transfer enhancement, fouling reducing and great mechanical stability [14]. The intricate network of pores and channels facilitates the efficient transport of molecules and ions across the membrane. Meanwhile, resistance to fluid flow and the effects of fouling are minimized. There are three different types of TPMS structure, which are: (1) Schwarz Primitive, (2) Schoen Gyroid and (3) Schwarz Diamond [15]. The Schwarz Primitive structure has the maximum compressive strength, with a mechanical resistance of 4.7 MPa, compared to the other two structures. Moreover, the Schwarz Primitive also has the lowest

* Corresponding to: Li Sze Lai (email: LaiLS@ucsiuniversity.edu.my)
DOI: https://doi.org/10.11113/jamst.v30n2.346

porosity percentage and the highest Young's modulus value. Due to the direct relationship among those parameters, the lower porosity with the higher Young's modulus and compressive strength will result in better mechanical behavior.

Femmer and co-workers successfully fabricated a PDMS membrane with a primitive TPMS architecture using rapid prototyping techniques [16]. The resulting membrane exhibited a selectivity comparable to that of conventional membranes. However, its permeability was about 15% lower, which was likely attributed to the high crosslinking density and relatively large membrane thickness (840 μm). In a subsequent study, Femmer *et al*. reported the fabrication of PDMS membranes using an acrylate-based sacrificial negative mold as a template for gas–liquid contacting applications [17]. The primitive TPMS structure demonstrated enhanced CO_2 transport performance. Moreover, computational fluid dynamics simulations revealed superior mass-transfer characteristics compared with hollow-fiber and flat-sheet membranes of similar geometric parameters. Although previous studies have demonstrated the feasibility of fabricating PDMS membranes with primitive TPMS architectures using rapid prototyping and sacrificial templating techniques, several research gaps remain. Existing studies mainly focused on pure PDMS membranes and evaluated the influence of the TPMS geometry on mass-transfer performance, particularly for gas–liquid contacting applications. However, limited attention has been given to the development of TPMS-based mixed-matrix membranes incorporating porous fillers to enhance CO_2 transport. Specifically, the incorporation of ZIF-8 nanoparticles into a primitive PDMS membrane structure has not been sufficiently investigated for pressure-driven CO_2 permeation. Furthermore, the relationship between filler incorporation, membrane morphology, thermal properties, and CO_2 permeation behaviour under different pressure differences remains unclear.

In this paper, a membrane with a primitive structure was fabricated for CO_2 permeation studies by incorporating 0.5 wt% ZIF-8 nanoparticles into the PDMS matrix. A loading of 0.5 wt.% was selected mainly because it has been reported as the optimum loading for CO_2 separation in the literature [18]. A sacrificial mold with a primitive structure was fabricated using the fused deposition modeling (FDM) method with Acrylonitrile Butadiene Styrene (ABS) material. Then, the mold was dissolved in the acetone to obtain the ZIF-8/PDMS membrane with the primitive structure. Subsequently, the membrane was examined for CO_2 permeation performance at different pressure differences. The ZIF-8 fillers and membrane were also characterized using Field Emission Scanning Electron Microscopy (FESEM) with Energy-Dispersive X-ray spectroscopy (EDX), Fourier transform infrared spectroscopy (FTIR), Differential Scanning Calorimetry (DSC), and Thermogravimetric Analysis (TGA).

2.0 METHODOLOGY

2.1 Synthesis of ZIF-8 Nanoparticles

The chemicals that were used for the fabrication of ZIF-8 nanoparticles were zinc nitrate hexahydrate ($Zn(NO_3)_2 \cdot 6H_2O$, 99%) as the source of zinc ion (Zn^{2+}), 2-methylimidazole (Hmim, 99%) as the organic ligand, and methanol (MeOH) as the solvent. 2.93 g of $Zn(NO_3)_2$ $6H_2O$ and 6.48 g of Hmim were weighed and dissolved separately in 200 mL of MeOH. They were then labeled as solution A and solution B, respectively. After that,

* Corresponding to: Li Sze Lai (email: LaiLS@ucsiuniversity.edu.my)
DOI: https://doi.org/10.11113/jamst.v30n2.346

solution B was added to solution A and rapidly mixed with a magnetic stirrer for 60 minutes at room temperature. During the process, a milky dispersion had been observed, indicating the crystallization of ZIF-8 nanoparticles. Then, the process was proceeded for centrifugation at 2500 rpm for 30 minutes. Next, the precipitate was rinsed with MeOH and centrifuged three more times to remove residues of unreacted reagents. The resulting particles was dried in the oven at 80°C for 3 hours. Pestle and mortar were used to grind the ZIF-8 nanoparticles into a fine powder.

2.2 Fabrication of Sacrificial Mold with Primitive Structure

The sacrificial mold was manufactured via the FDM method using ABS with 100% filler content. The mold was designed with 2 × 1 × 1 cubic unit cell of sheet-like primitive structure. Figure 1 shows the CAD drawing and the printed sacrificial mold.

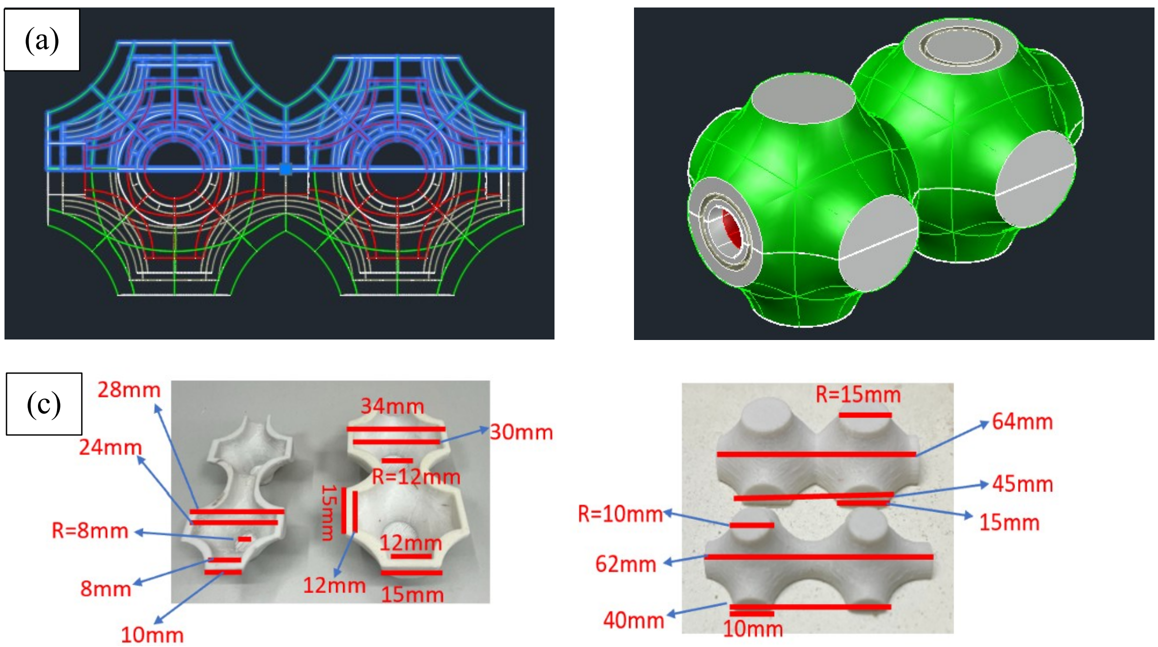

Figure 1. (a) Top view of primitive-structure sacrificial mold; (b) 3D view of primitive-structure sacrificial mold; (c) ABS sacrificial mold printed via FDM

2.3 Fabrication of ZIF-8/PDMS Membrane with Primitive Structure

In this paper, a ZIF-8/PDMS membrane was fabricated with a primitive structure as one of the TPMS structures. 0.5 wt% of ZIF-8 nanoparticles were dispersed in PDMS pre-polymer base (Sylgard 184), and the mixture was stirred continuously at constant speed for 1 hour to ensure homogeneous distribution of the nanoparticles. The resulting suspension was then sonicated at 50 W for 30 minutes to further improve nanoparticle dispersion and minimize agglomeration. After sonication, the curing agent was added to the mixture, followed by an additional 30 minutes of stirring at constant speed to ensure uniform mixing. To remove entrapped air bubbles, the mixture was subjected to vacuum treatment for 30 minutes. The degassed solution was then injected into a primitive

* Corresponding to: Li Sze Lai (email: LaiLS@ucsiuniversity.edu.my)
DOI: https://doi.org/10.11113/jamst.v30n2.346

sacrificial mold to form ZIF-8/PDMS membranes. A stick was glued on top of the mold to achieve a uniform membrane thickness. The membranes were dried at room temperature for 3 days to allow partial curing, followed by thermal treatment in a conventional oven at 60 °C for an additional 3 days to complete the curing process. Then, the sacrificial mold was dissolved in AR-grade acetone (≥99.5%) for 24 hours. After removing the residual ABS sacrificial mold on the membrane surface, the membrane was cleaned and dried overnight. Two parts of the membrane were then combined using super-strong epoxy adhesive (Araldite brand).

2.4 Characterization of ZIF-8 Nanoparticles and ZIF-8/PDMS Membrane

The ZIF-8 nanoparticles were characterized using FESEM, FTIR, XRD and TGA. The resultant membrane was characterized using FESEM coupled with EDX, FTIR, XRD, and DSC. The FESEM, coupled with EDX, was conducted using the brand Tescan and the model Clara. The FTIR was conducted using Perkin Elmer (Spectrum Two). The XRD analysis was conducted using a PANalytical Empyrean. The scanning was conducted using Cu Kα radiation (λ = 1.540 Å) at 40 mA and 45 kV, from 5º to 90º in 0.026º steps. The TGA was measured using a TA Instruments model Q50 at a heating rate of 10.00 °C/min to 800 °C. The DSC was tested using Netzsch Brand, Netzsch DSC 214 Polyma. The temperature was ranged from -120 °C to 30 °C at heating rate of 10 °C/min and nitrogen gas flow rate of 40 ml/min.

2.5 Gas Permeation Testing of Membrane

The ZIF-8/PDMS membrane was examined for its gas permeation performance using a constant-pressure system at room temperature. The gas feed, consisting of pure CO_2 (min 99.8%) or N_2 (min 99.999%), was introduced into a membrane cell module with a primitive structure. The feed pressure of the system was measured using a pressure gauge, and the inlet gas flow rate of 0.125 L/min was regulated using a rotameter. The pressure difference of the system was controlled using a back-pressure regulator, which was varied from 0.025 bar to 0.15 bar. The gas on the permeate side was connected to a bubble flowmeter for flow-rate measurement. The permeate flow rate and standard deviation were calculated from the repeated measurements using different membranes for the reproducibility test. The permeability, P_{CO_2} (mol·m/m^2·s·Pa) of the gas was estimated using the Equation 1:

$$P_{CO_2} = \frac{N_{CO_2} l}{\Delta P_{CO_2}} \quad (1)$$

where N_{CO_2} is the flux (mol m^{-2} s^{-1}), l is membrane thickness (m) and ΔP is the pressure difference (Pa). Noted that 1 barrer is equivalent to 3.348×10^{-16} mol·m/ (m^2·s·Pa). Then, the ideal selectivity for CO_2 and N_2 was calculated as the ratio of the gas permeability by using Equation 2:

$$\alpha_{CO_2/N_2} = \frac{P_{CO_2}}{P_{N_2}} \quad (2)$$

* Corresponding to: Li Sze Lai (email: LaiLS@ucsiuniversity.edu.my)
DOI: https://doi.org/10.11113/jamst.v30n2.346

©Universiti Teknologi Malaysia

Figure 2 shows the primitive-structured membrane placed in the custom-made membrane cell for gas permeation testing. A needle from syringe was connected to the membrane outlet (permeate) using a silicone stopper.

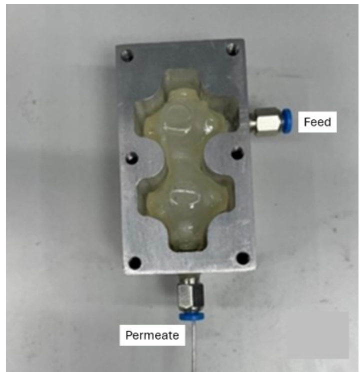

Figure 2. Gas permeation testing using primitive-structured ZIF-8/PDMS membrane placed in a custom-made membrane module with primitive shape

3.0 RESULTS AND DISCUSSION

The ZIF-8 nanoparticles and ZIF-8/PDMS membrane were successfully synthesized and characterized using FESEM, EDX, FTIR, XRD, DSC, and TGA. Subsequently, CO_2 and N_2 gas permeation across ZIF-8/PDMS has also been investigated.

3.1 Characterization of ZIF-8 Nanoparticles and ZIF-8/PDMS Membrane

Figure 3 shows the FESEM images of ZIF-8 nanoparticles, ZIF-8/PDMS membrane with 0.5 wt% loading of ZIF-8 particles and pristine PDSM membrane. As shown in the FESEM images, ZIF-8 nanoparticles with sizes ranging from 46 to 62 nm were successfully synthesized. In addition, the ZIF-8 nanoparticles were mostly uniformly dispersed on the membrane surface and embedded within the polymeric matrix. However, small agglomeration was not able to be avoided and can be observed from Figure 3. Sonication time can be increased further to prevent agglomeration.

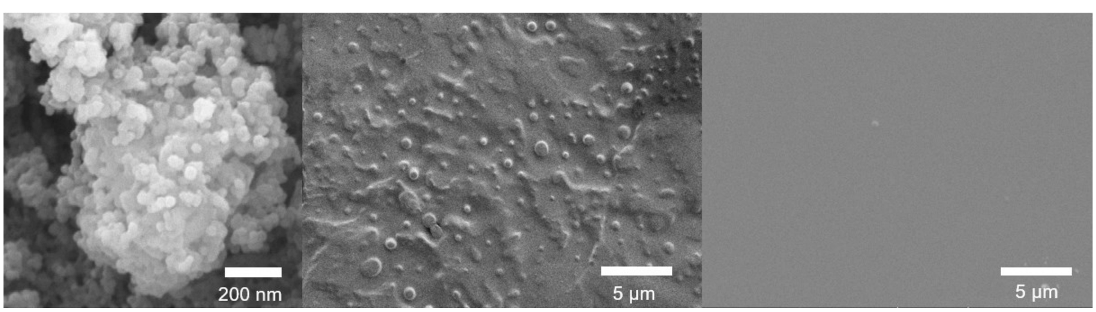

Figure 3. FESEM image of (left) ZIF-8 nanoparticles; (middle) ZIF-8/PDMS membrane and (right) pristine PDMS membrane

* Corresponding to: Li Sze Lai (email: LaiLS@ucsiuniversity.edu.my)
DOI: https://doi.org/10.11113/jamst.v30n2.346

Table 1 shows the EDX composition of ZIF-8 nanoparticles, ZIF-8/PDMS and pristine PDMS membranes. Referring to Table 1, the ZIF-8 nanoparticles show the composition of C, N, and Zn, with Zn detected at 27.30 wt%. This has indicating the formation of high-purity ZIF-8, in which C and N were mainly contributed by the imidazole organic linker, and Zn was mainly contributed by the zinc metal ion. The result is consistent with the literature [19]. For the pristine PDMS membrane, C, O, and Si were detected at 37.64, 30.41, and 31.95 wt%, respectively. These elements were consistent with the chemical structure of PDMS, which contained organic methyl groups and a siloxane backbone. For the ZIF-8/PDMS membrane, the main elements detected were C, O, and Si, with values of 36.72, 30.38, and 31.96 wt%, respectively. These values were very close to those of pristine PDMS, indicating that PDMS remained the dominant matrix phase in the membrane. The detection of Zn at 0.85 wt% confirmed the successful incorporation of ZIF-8 into the PDMS membrane. However, the Zn content should be interpreted as a local surface composition rather than the exact bulk filler loading, because EDX is a localized and semi-quantitative technique. The trace amount of Na at 0.09 wt% may be due to minor surface contamination, residual impurity, or spectral overlap, and is considered negligible.

Table 1. EDX composition of ZIF-8 nanoparticles, ZIF-8/PDMS and pristine PDMS membranes

Elements	Weight %		
	ZIF-8 nanoparticles	ZIF-8/PDMS membrane	PDMS membrane
C	47.36	36.72	37.64
N	21.91	-	-
O	3.44	30.38	30.41
Si	-	31.96	31.95
Zn	27.30	0.85	-
Na	-	0.09	-
Total	100.0	100.0	100.0

FTIR characterization was conducted to determine the main wavenumber peaks and their corresponding functional groups. Figure 4 shows the FTIR characterization result of ZIF-8 nanoparticles. Characteristics peaks of ZIF-8 were observed at 421 cm^{-1}, 1148 cm^{-1}, 1584 cm^{-1}, 2931 cm^{-1} and 3136 cm^{-1}, which are consistent with the characteristic peaks of ZIF-8 reported in the literature [20]. Noted that the peaks at 2931 cm^{-1} and 3136 cm^{-1} were relatively weak, assigned to the N-H (amide) group and C-H (alkane) stretching group of imidazole, respectively. Meanwhile, the peak at 1584 cm^{-1} was attributed to the C = N stretch mode and the peak at 421 cm^{-1} was due to the Zn-N stretching mode. In addition, the peak at 1148 cm^{-1} was the main characteristics peak for ZIF-8, which was caused by the C-N stretching.

The FTIR analysis of pristine PDMS and ZIF-8/PDMS membranes were also compared in Figure 4. The results are consistent with the literature data [21]. For the PDMS

* Corresponding to: Li Sze Lai (email: LaiLS@ucsiuniversity.edu.my)
DOI: https://doi.org/10.11113/jamst.v30n2.346

membrane, the characteristic bands included the Si–O–Si stretching (~1019 cm^{-1}), the Si–CH_3 deformation (~1246 cm^{-1}), and the Si–C/Si–O–Si bending (~873 cm^{-1}). The absorption in the region 2769–3000 cm^{-1} corresponded to the aliphatic C–H stretching vibrations of methyl groups. Both pristine and ZIF-8/PDMS membranes showed almost identical FTIR spectra, mainly due to the low wt% of ZIF-8 incorporated, where the dominant PDMS bands eclipsed the characteristic vibrations of ZIF-8.

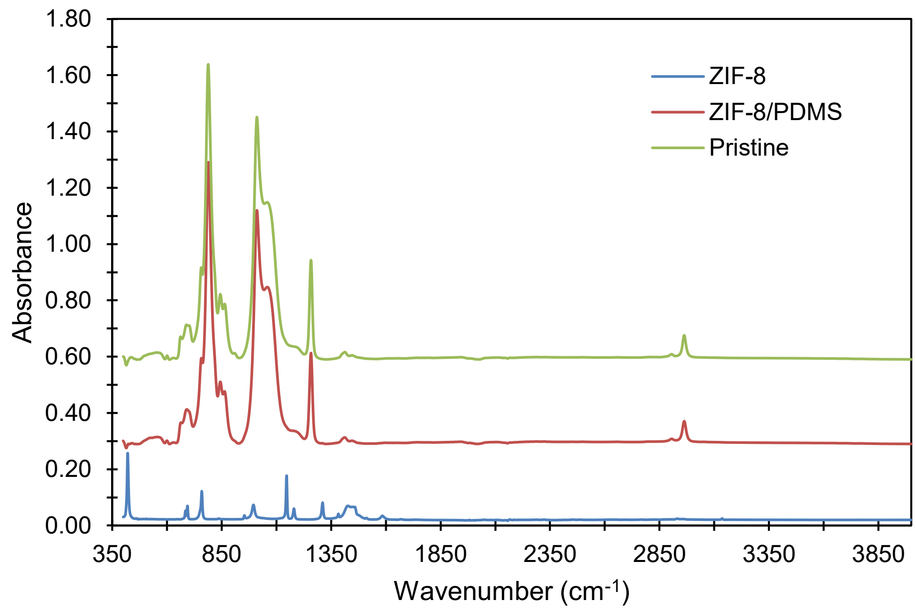

Figure 4. FTIR spectrum of ZIF-8, ZIF-8/PDMS and pristine membranes

Figure 5 shows the XRD patterns of the ZIF-8 nanoparticles and ZIF-8/PDMS membranes. It can be seen that high-purity ZIF-8 nanoparticles have been successfully synthesized in this study, as evidenced by the presence of all characteristic peaks [22]. The nanoparticles showed high crystallinity with a sharp (011) peak at 7.3°. The XRD result is consistent with the FESEM image, in which the ZIF-8 nanoparticles were shown to be cubic or hexagonal with edges. For the ZIF-8/PDMS membrane, a weak peak was observed at 11.64°, mainly due to the amorphous nature of the PDMS matrix [23]. Noted that due to the low wt % of ZIF-8 loading, the characteristic peaks of ZIF-8 can be hardly observed from the XRD pattern of the ZIF-8/PDMS membrane.

* Corresponding to: Li Sze Lai (email: LaiLS@ucsiuniversity.edu.my)
DOI: https://doi.org/10.11113/jamst.v30n2.346

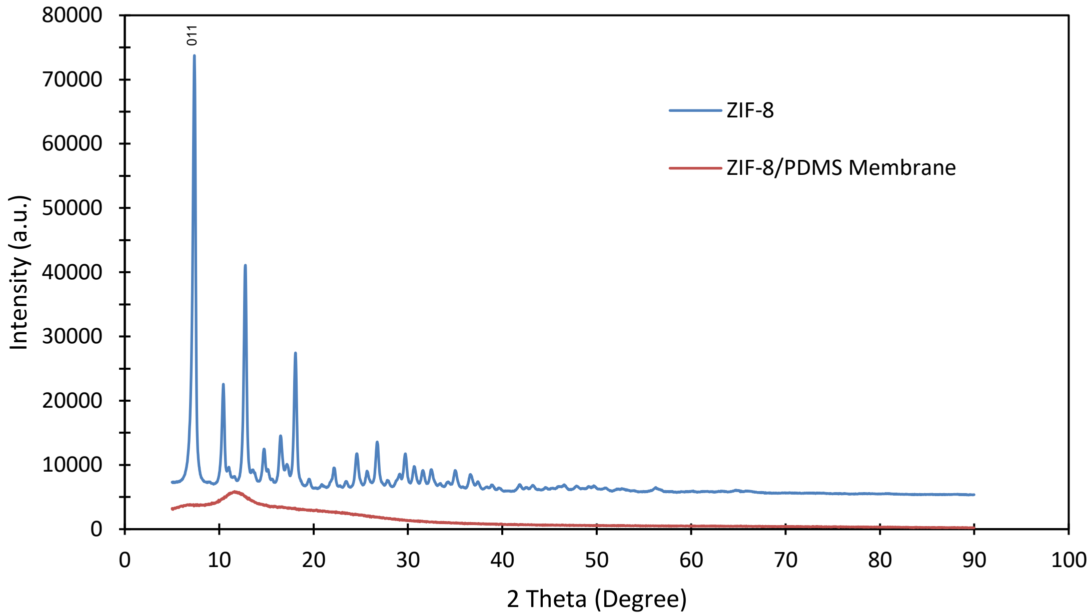

Figure 5. XRD pattern of ZIF-8 and ZIF-8/PDMS membrane

Figure 6 shows the TGA graph result of ZIF-8 nanoparticles. The result is consistent with the literature [24]. A small weight loss of 12.31% was observed when the temperature increased to 300 °C. This was mainly due to the removal of solvent molecules (methanol) from the cavities and of some 2-methylimidazolate species from the particle surfaces. Further mass loss up to 700 °C was mainly due to the removal of organic linker molecules. Eventually, the residual mass (about 25.74%) after 700 °C was due to the formation of zinc oxide (ZnO). The TGA result demonstrated that the ZIF-8 nanoparticles have high purity.

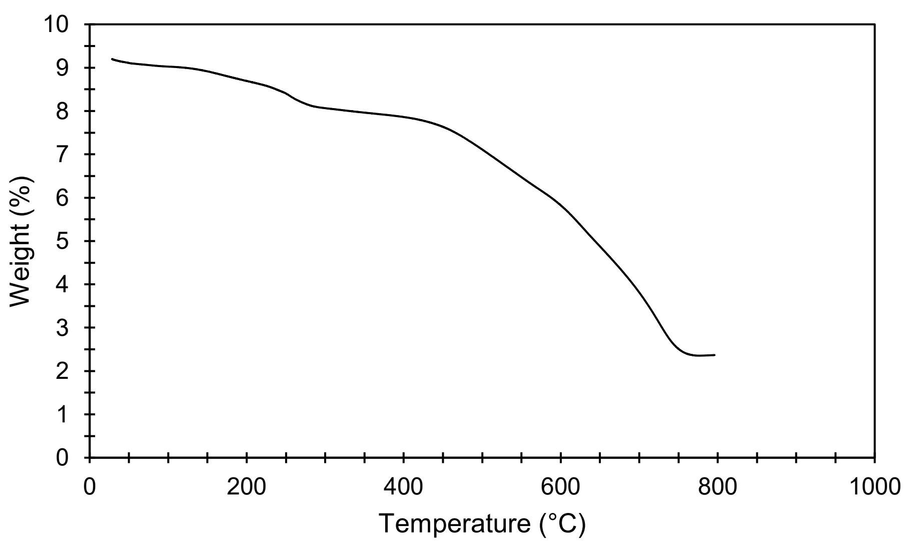

Figure 6. TGA graph result of ZIF-8 nanoparticles

* Corresponding to: Li Sze Lai (email: LaiLS@ucsiuniversity.edu.my)
DOI: https://doi.org/10.11113/jamst.v30n2.346

Figure 7 shows the DSC results for the fabricated pristine PDMS and ZIF-8/PDMS membranes. For the pristine PDMS membrane, the glass transition temperature (Tg) was measured at approximately –104.2 °C. This result is consistent with the literature, where Klonos *et al*. reported that the Tg of PDMS is typically below –100 °C [25]. The agreement between the experimental and reported values indicate that the pristine PDMS membrane was fabricated appropriately. For the ZIF-8/PDMS membrane, the first observed Tg was comparable to that of pristine PDMS, suggesting that the incorporation of ZIF-8 nanoparticles does not significantly alter the intrinsic Tg of the PDMS matrix. However, the DSC curve of the ZIF-8/PDMS membrane showed additional transitions, which were reflected by multiple peaks. The presence of multiple peaks indicated a heterogeneous system, consistent with the fact that the membrane is a composite of ZIF-8 nanoparticles and PDMS polymer [26]. Specifically, additional thermal transitions were observed at –72 °C and –44.8 °C, which can be attributed to the crystallization temperature (Tc) and melting temperature (Tm) of the ZIF-8/PDMS membrane, respectively. These results align with those reported by Fang *et al*., where a 5 wt% ZIF-8/PDMS membrane exhibited Tc and Tm at approximately –73 °C and –44 °C [27]. Therefore, the DSC results confirm that the ZIF-8/PDMS membrane was fabricated successfully and that its thermal properties are consistent with the literature.

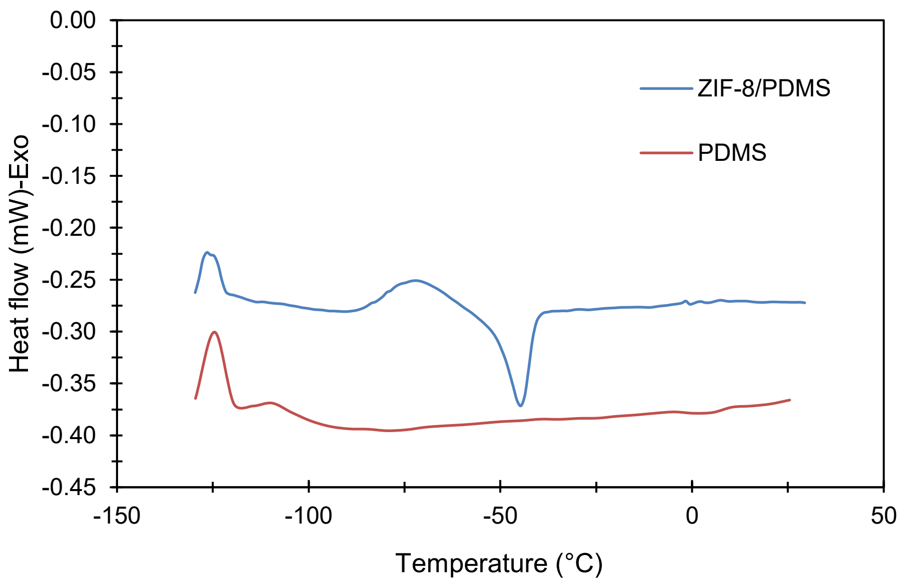

Figure 7. DSC result of the fabricated pristine PDMS and ZIF-8/PDMS membrane

3.2 Gas Permeation Testing

Figure 8 shows the CO_2 and N_2 permeability of a primitive-structured ZIF-8/PDMS membrane at pressure differences ranging from 0.025 bar to 0.15 bar at room temperature. From Figure 8, it can be seen that for the primitive-structure ZIF-8/PDMS membrane, CO_2 permeability decreases slightly from $13.17 \pm 0.57 \times 10^3$ barrer to $9.78 \pm 0.28 \times 10^3$ barrer as the pressure difference increases from 0.025 bar to 0.15 bar. This trend might be due to the incorporation of ZIF-8 fillers into the soft PDMS matrix that may generate microscopic

* Corresponding to: Li Sze Lai (email: LaiLS@ucsiuniversity.edu.my)
DOI: https://doi.org/10.11113/jamst.v30n2.346

©Universiti Teknologi Malaysia

interfacial voids at the polymer–filler boundary. Then, at very low driving forces, such as 0.025 bar, penetrant CO_2 gas molecules can rapidly occupy these localized voids, and hence, causing a temporary increase in the apparent permeability. However, as the pressure increases towards 0.15 bar, these specific sorption sites may become progressively saturated. Gas transport then becomes increasingly governed by the conventional solution–diffusion process within the bulk PDMS matrix, resulting in a decrease in permeability [28]. The trend is consistent with those reported in the literature [29]. Meanwhile, N_2 permeability remains almost constant with a slight reduction from $1.70 \pm 0.04 \times 10^3$ barrer to $0.68 \pm 0.02 \times 10^3$ barrer when the pressure varied from 0.025 bar to 0.15 bar. Additionally, the membrane demonstrated an ideal CO_2/N_2 selectivity of 7.76 ± 0.28 at a pressure difference of 0.025 bar.

The CO_2 permeability is higher than that reported for PDMS-based membranes in the literature, which is 5202.10 barrer, but the CO_2/N_2 selectivity is lower than that reported at 10.50 [13]. However, both of them were lower as compared with the CO_2 permeability and CO_2/N_2 selectivity reported for a ZIF-8/PDMS membrane supported on a mullite-based substrate with 0.8 wt.% ZIF-8 loading, which reached 4.58×10^4 barrer and 10.7, respectively, at feed pressure of 2 bar [12]. In general, the observed CO_2 permeability was within a comparable order of magnitude to values reported for ZIF-8/PDMS membranes in the literature, although differences in membrane thickness, filler loading, and fabrication configuration may contribute to variations in performance.

The lower CO_2/N_2 selectivity further suggests that the current membrane configuration may not fully exploit the molecular sieving or preferential CO_2 transport contribution of ZIF-8. This may be attributed to the relatively thick PDMS matrix and the associated increase in gas transport resistance. Nevertheless, the membrane still maintained CO_2-selective behaviour. It is plausible that the dissolution process of the sacrificial mold by using acetone did not introduce major non-selective defects into the membrane structure. Hence, this method can serve as a feasible route for fabricating structured and rubbery PDMS-based membranes for gas separation study.

Figure 9 shows the results of the current study compared with other membranes reported for CO_2/N_2 separation. It can be observed that the membrane performance has not yet surpassed the Robeson Upper Bound limit. At present, the primitive-structured membrane is relatively thick, about 1 mm, owing to the design of the sacrificial mold. This thickness may impose substantial resistance to gas transport across the membrane matrix. As a result, the CO_2 permeability of the pristine PDMS membrane (16.286×10^3 barrer at 0.025 bar) did not differ markedly from that of the ZIF-8/PDMS membrane. This suggests that the gas transport behaviour was mainly governed by the membrane thickness and PDMS matrix resistance, while the contribution of ZIF-8 to enhancing CO_2 permeability may be limited under the current membrane configuration.

* Corresponding to: Li Sze Lai (email: LaiLS@ucsiuniversity.edu.my)
DOI: https://doi.org/10.11113/jamst.v30n2.346

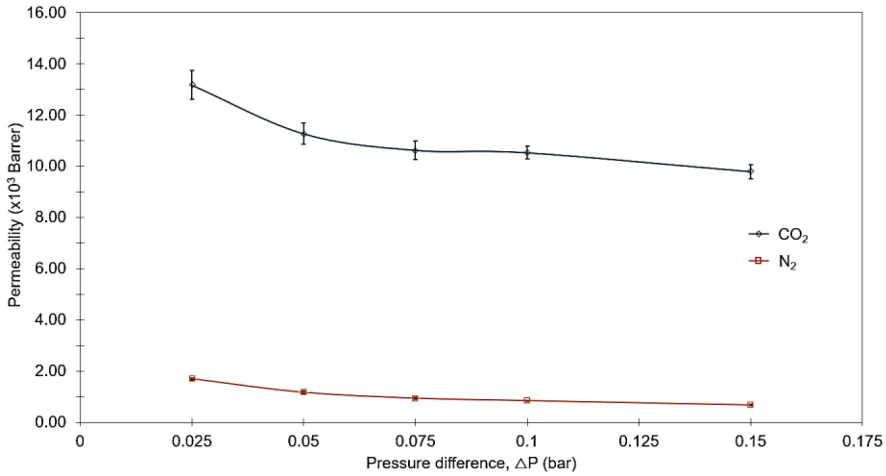

Figure 8. CO_2 and N_2 permeability of primitive-structured ZIF-8/PDMS membrane against pressure differences ranged from 0.025 bar to 0.15 bar at room temperature

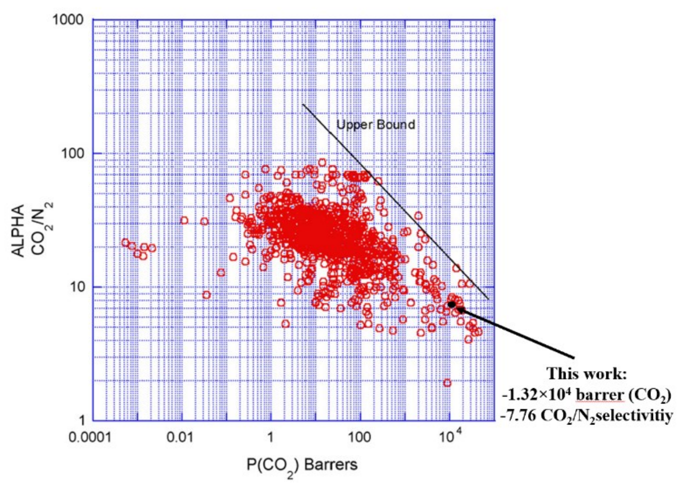

Figure 9. Result comparison with Robenson Upper Bound [30]

4.0 CONCLUSION

In conclusion, high-purity ZIF-8 nanoparticles were successfully synthesized, and their characteristics were examined using FESEM, EDX, FTIR, XRD, and TGA. The characterization results confirmed that highly crystalline nanoscale ZIF-8 was appropriately synthesized. In addition, both PDMS and ZIF-8/PDMS membranes with primitive structures were fabricated. The membrane characteristics were also analyzed using FESEM, EDX, FTIR, XRD, and DSC, showing a uniform distribution of ZIF-8 nanoparticles. Subsequently, the ZIF-8/PDMS membrane was subjected to CO_2 and N_2 pure gas permeation testing. The primitive-structured ZIF-8/PDMS membrane exhibited CO_2 permeability and CO_2/N_2 ideal selectivity that are comparable to reported literature values, which are $13.17 \pm 0.57 \times 10^3$ Barrer and 7.76 ± 0.28, respectively, at a pressure difference of 0.025 bar. These results indicate that membrane quality is not compromised by the sacrificial mold's dissolution. However, the current membrane performance has yet

* Corresponding to: Li Sze Lai (email: LaiLS@ucsiuniversity.edu.my)
DOI: https://doi.org/10.11113/jamst.v30n2.346

to surpass the Robeson Upper Bound, possibly due to membrane thickness, which could be further reduced by introducing a porous support layer. Overall, this study provides significant insight into the fabrication of complex-structured membranes using additive manufacturing methods.

The sacrificial mold fabrication method shows good scalability because it relies on a removable template to define complex 3D architectures. This approach allows the fabrication of membranes with controlled geometry, interconnected channels, and high surface-area structures that are difficult to obtain using conventional flat-sheet membrane casting. For larger-scale production, the method could be adapted through batch mold printing, although challenges such as mold removal, solvent use, dimensional consistency, and fabrication time must be carefully managed.

Industrially, sacrificial mold fabrication has strong potential for applications requiring structured membranes with enhanced mass transfer, such as CO_2 separation, biogas upgrading, gas purification, membrane contactors, and solvent-resistant separations. The method is also relevant for producing customized membrane modules, microfluidic separation devices, and catalytic or adsorptive supports. Its ability to create well-defined porous or TPMS-like structures makes it promising for advanced separation systems where high permeability, controlled flow pathways, and reduced pressure drop are required.

DECLARATION OF COMPETING INTEREST

The authors declare that they have no known competing financial interests or personal relationships that could have appeared to influence the work reported in this paper.

ACKNOWLEDGEMENTS

The study was funded by the Malaysian Ministry of Higher Education through the Fundamental Research Grant Scheme (FRGS/1/2023/TK09/UCSI/03/1) and UCSI University, KL Campus through UCSI Research Excellence & Innovation Grant (REIG) (REIG-FETBE-2023/017).

REFERENCES

[1] Guan, W., Dai, Y., Dong, C., Yang, X., & Xi, Y. (2020). Zeolite imidazolate framework (ZIF)-based mixed matrix membranes for CO_2 separation: A review. *Journal of Applied Polymer Science, 137*, 48968.

[2] Ti, W., Ng, D. K., Ng, L. Y., & Andiappan, V. (2022). Optimal blue hydrogen process with CO_2 capture, utilisation and storage. *Chemical Engineering Transactions, 94*, 211–216.

[3] Rangaraj, V. M., Wahab, M. A., Reddy, K. S. K., Kakosimos, G., Abdalla, O., Favvas, E. P., *et al.* (2020). Metal organic framework-based mixed matrix membranes for carbon dioxide separation: Recent advances and future directions. *Frontiers in Chemistry, 8*. https://doi.org/10.3389/fchem.2020.00534

[4] Lei, L., Bai, L., Lindbråthen, A., Pan, F., Zhang, X., & He, X. (2020). Carbon membranes for CO_2 removal: Status and perspectives from materials to processes. *Chemical Engineering Journal, 401*, 126084.

* Corresponding to: Li Sze Lai (email: LaiLS@ucsiuniversity.edu.my)
DOI: https://doi.org/10.11113/jamst.v30n2.346

https://doi.org/10.1016/j.cej.2020.126084
[5] Kamble, A. R., Patel, C. M., & Murthy, Z. V. P. (2021). A review on the recent advances in mixed matrix membranes for gas separation processes. *Renewable and Sustainable Energy Reviews, 145*, 111062. https://doi.org/10.1016/j.rser.2021.111062
[6] Katare, A., Kumar, S., Kundu, S., Sharma, S., Kundu, L. M., & Mandal, B. (2023). Mixed matrix membranes for carbon capture and sequestration: Challenges and scope. *ACS Omega, 8*, 17511–17522. https://doi.org/10.1021/acsomega.3c00976
[7] Nguyen, T.-M. T., Chen, J.-W., Pham, M.-T., Bui, H. M., Hu, C.-C., You, S.-J., *et al*. (2023). A high-performance ZIF-8 membrane for gas separation applications: Synthesis and characterization. *Environmental Technology & Innovation, 31*, 103169. https://doi.org/10.1016/j.eti.2023.103169
[8] Ashtiani, S., Sofer, Z., Průša, F., & Friess, K. (2021). Molecular-level fabrication of highly selective composite ZIF-8-CNT-PDMS membranes for effective CO2/N2, CO2/H2 and olefin/paraffin separations. *Separation and Purification Technology, 274*, 119003. https://doi.org/10.1016/j.seppur.2021.119003
[9] Cao, Q., Ding, X., Zhao, H., Zhang, L., Xin, Q., & Zhang, Y. (2021). Improving gas permeation performance of PDMS by incorporating hollow polyimide nanoparticles with microporous shells and preparing defect-free composite membranes for gas separation. *Journal of Membrane Science, 635*, 119508. https://doi.org/10.1016/j.memsci.2021.119508
[10] Taherizadeh, A., Simon, A., Richter, H., Stelter, M., & Voigt, I. (2024). Development and investigation of a multilayer PDMS/zeolite composite membrane for CO_2 separation applications. *Separation and Purification Technology, 346*, 127344. https://doi.org/10.1016/j.seppur.2024.127344
[11] Wang, H., Ni, Y., Dong, Z., & Zhao, Q. (2021). A mechanically enhanced metal-organic framework/PDMS membrane for CO_2/N_2 separation. *Reactive and Functional Polymers, 160*, 104825. https://doi.org/10.1016/j.reactfunctpolym.2021.104825
[12] Fu, W., Zhang, L., Liu, J., Yang, T., Sun, M., Ma, X., *et al.* (2025). Ceramic-based composite membranes decorated by incorporating ZIF-8 and PDMS for highly efficient CO_2/N_2 separation. *Separation and Purification Technology, 352*, 128142. https://doi.org/10.1016/j.seppur.2024.128142
[13] Gutierrez, D. B., Caldona, E. B., Yang, Z., Suo, X., Cheng, X., Dai, S., *et al.* (2022). 3D-printed PDMS-based membranes for CO_2 separation applications. *MRS Communications, 12*, 1174–1182. https://doi.org/10.1557/s43579-022-00285-0
[14] Thomas, N., Sreedhar, N., Al-Ketan, O., Rowshan, R., Abu Al-Rub, R. K., & Arafat, H. (2019). 3D printed spacers based on TPMS architectures for scaling control in membrane distillation. *Journal of Membrane Science, 581*, 38–49. https://doi.org/10.1016/j.memsci.2019.03.059
[15] Novak, N., Al-Ketan, O., Krstulović-Opara, L., Rowshan, R., Abu Al-Rub, R. K., Vesenjak, M., *et al*. (2021). Quasi-static and dynamic compressive behaviour of sheet TPMS cellular structures. *Composite Structures, 266*, 113801. https://doi.org/10.1016/j.compstruct.2021.113801
[16] Femmer, T., Kuehne, A. J. C., & Wessling, M. (2014). Print your own membrane: Direct rapid prototyping of polydimethylsiloxane. *Lab on a Chip, 14*, 2610–2613.

* Corresponding to: Li Sze Lai (email: LaiLS@ucsiuniversity.edu.my)
DOI: https://doi.org/10.11113/jamst.v30n2.346

https://doi.org/10.1039/C4LC00471B
[17] Femmer, T., Kuehne, A. J. C., Torres-Rendon, J., Walther, A., & Wessling, M. (2015). Print your membrane: Rapid prototyping of complex 3D-PDMS membranes via a sacrificial resist. *Journal of Membrane Science, 478*, 12–18. https://doi.org/10.1016/j.memsci.2014.12.038
[18] Md. Nordin, N. A. H., Ismail, A. F., Mustafa, A., Murali, R. S., & Matsuura, T. (2015). Utilizing low ZIF-8 loading for an asymmetric PSf/ZIF-8 mixed matrix membrane for CO2/CH4 separation. *RSC Advances, 5*, 30206–30215. https://doi.org/10.1039/C5RA01856B
[19] Zhang, H., Zhao, M., Yang, Y., & Lin, Y. S. (2019). Hydrolysis and condensation of ZIF-8 in water. *Microporous and Mesoporous Materials, 288*, 109568. https://doi.org/10.1016/j.micromeso.2019.109568
[20] Liu, J., He, J., Wang, L., Li, R., Chen, P., Rao, X., *et al*. (2016). NiO-PTA supported on ZIF-8 as a highly effective catalyst for hydrocracking of *Jatropha* oil. *Scientific Reports, 6*, 23667. https://doi.org/10.1038/srep23667
[21] Bourassi, M., Pasichnyk, M., Oesch, O., Sundararajan, S., Trávničková, T., Soukup, K., *et al.* (2021). Glycidyl and methyl methacrylate UV-grafted PDMS membrane modification toward tramadol membrane selectivity. *Membranes, 11*, 752. https://doi.org/10.3390/membranes11100752
[22] Du, P. D., Hieu, N. T., & Thien, T. V. (2021). Ultrasound-assisted rapid ZIF-8 synthesis, porous ZnO preparation by heating ZIF-8, and their photocatalytic activity. *Journal of Nanomaterials, 2021*, 9988998. https://doi.org/10.1155/2021/9988998
[23] Pan, Y., Xie, R., Xu, B., & Chen, C. (2021). Determination of sorption and diffusion for ethanol through superhydrophobic ZIF/PDMS mixed matrix membrane. *Microporous and Mesoporous Materials, 320*, 111086. https://doi.org/10.1016/j.micromeso.2021.111086
[24] Mohammadi, A., & Nakhaei Pour, A. (2023). Triethylenetetramine-impregnated ZIF-8 nanoparticles for CO_2 adsorption. *Journal of CO_2 Utilization, 69*, 102424. https://doi.org/10.1016/j.jcou.2023.102424
[25] Klonos, P. A. (2018). Crystallization, glass transition, and molecular dynamics in PDMS of low molecular weights: A calorimetric and dielectric study. *Polymer, 159*, 169–180. https://doi.org/10.1016/j.polymer.2018.10.069
[26] TA Instruments. (2023). *Interpreting DSC curves: Part 1—Dynamic measurements*. https://www.tainstruments.com/
[27] Fang, M., Wu, C., Yang, Z., Wang, T., Xia, Y., & Li, J. (2015). ZIF-8/PDMS mixed matrix membranes for propane/nitrogen mixture separation: Experimental result and permeation model validation. *Journal of Membrane Science, 474*, 103–113. https://doi.org/10.1016/j.memsci.2014.09.050
[28] Li, S., Li, Z., & Dong, Q. (2016). Diffusion coefficients of supercritical CO_2 in oil-saturated cores under low permeability reservoir conditions. *Journal of CO_2 Utilization, 14*, 47–60. https://doi.org/10.1016/j.jcou.2016.03.002
[29] Zainuddin, M. I. F., Ahmad, A. L., & Shah Buddin, M. M. H. (2023). Polydimethylsiloxane/magnesium oxide nanosheet mixed matrix membrane for CO_2 separation application. *Membranes, 13*, 337. https://doi.org/10.3390/membranes13030337

* Corresponding to: Li Sze Lai (email: LaiLS@ucsiuniversity.edu.my)
DOI: https://doi.org/10.11113/jamst.v30n2.346

©Universiti Teknologi Malaysia

[30] Robeson, L. M. (2008). The upper bound revisited. *Journal of Membrane Science, 320*, 390–400. https://doi.org/10.1016/j.memsci.2008.04.030

* Corresponding to: Li Sze Lai (email: LaiLS@ucsiuniversity.edu.my)
DOI: https://doi.org/10.11113/jamst.v30n2.346